MIT Open Access Articles

Resonant-cavity enhanced thermal emission

Resonant-cavity enhanced thermal emission

Ivan Celanovic,* David Perreault, and John Kassakian

Laboratory for Electromagnetic and Electronic Systems, Massachusetts Institute of Technology, Cambridge, Massachusetts 02139, USA
(Received 16 June 2005; published 19 August 2005)

In this paper we present a vertical-cavity enhanced resonant thermal emitter—a highly directional, narrow-band, tunable, partially coherent thermal source. This device enhances thermal emittance of a metallic or any other highly reflective structure to unity near a cavity resonant frequency. The structure consists of a planar metallic surface (e.g., silver, tungsten), a dielectric layer on top of the metal that forms a vertical cavity, followed by a multilayer dielectric stack acting as a partially transparent cavity mirror. The resonant frequency can easily be tuned by changing the cavity thickness (thus shifting resonant emission peak), while the angle at which the maximum emittance appears can be tuned as well by changing the number of dielectric stack layers. The thermal emission exhibits an extremely narrow angular emission lobe, suggesting increased spatial coherence. Furthermore, we show that we can enhance the thermal emission of an arbitrarily low-emittance material, choosing a properly designed thermal cavity, to near unity.

I. INTRODUCTION

Bulk thermal emission sources are commonly perceived as isotropic, broadband, and incoherent electromagnetic radiation sources. Although different bulk materials exhibit different emission characteristics, tailoring emission properties require engineering new material systems and structures that interact with sources of radiation—fluctuating thermal sources—on a wavelength scale. Indeed, structures with feature sizes on the order of radiation wavelengths—such as photonic crystals (PhC)—exhibit qualitatively different radiation behavior due to intricate interaction between the radiation and the matter. The ability to modulate photonic density of states and hence modify spontaneous emission rates in photonic crystals[1] opens immense possibilities for designing novel thermal sources.

One-dimensional photonic crystals, for example, can significantly suppress thermal radiation for a range of frequencies (in the band gap) while enhancing radiation outside the band gap.[2–4] Two-dimensional (2D) photonic crystals can be designed to enhance emittance for a range of frequencies.[5–7] Furthermore, three-dimensional (3D) photonic crystals exhibit a complete band gap which results in a large emission stop band, while the emittance is significantly enhanced in the vicinity of the band edge.[8,9] The increased density of photonic states near the band edge suggests increased coherence length of the emitted radiation, however, this has not been investigated in the literature.

The majority of the published work on thermal radiation properties of 1D, 2D, and 3D photonic crystals investigates the suppression and enhancement of thermal emission for a wide range of wavelengths. However, in this work we are particularly interested in narrow-band, antennalike thermal emission from PhC structures. Previously, it was shown that surface patterned materials (with surface grating or 2D photonic crystal) that support surface polaritons (plasmon-polariton or phonon-polariton) can have narrow angular and narrow-band thermal radiation properties resulting in increased spatial and temporal coherence in the far field.[10–12] Thermal emission properties of these structures allow certain degrees of freedom in adjusting the emission peak wavelength and directionality. Antennalike emission patterns were also noticed with even simple planar structures such as thin-film emitters.[13] In 3D tungsten PhC,[9] strong resonant enhancement near the band edge was observed which also suggests increased spatial coherence. Yet this structure shows a large emissivity outside the photonic band gap which makes it unsuitable for applications that require highly selective emission properties.

In this paper we present a thermal emitter—quasimonochromatic, highly directional, with tunable emission peak resonance and tunable directionality—named a vertical-cavity enhanced resonant thermal emitter (VERTE). Our initial motivation was to use an optical cavity resonance to resonantly enhance thermal noise generated by fluctuating thermal sources in the cavity while suppressing it elsewhere. The design was inspired by the vertical cavity surface emitting laser (VCSEL).[14] However, unlike the VCSEL, where the active medium is embedded in the cavity between the two 1D photonic crystals, the VERTE consists of a cavity sandwiched between partially reflective 1D PhC on one side and a highly reflective metallic mirror on the other side, as shown in Fig. 1. Ideally, the 1D PhC and the cavity are lossless (they are highly transparent in the range of wavelengths that are of interest) while the metallic mirror is highly reflective yet slightly absorbing—thus acting as both the high-temperature source of radiation and the cavity mirror. The cavity, with its strong frequency dependant transfer function, enhances thermal emission originating from the metallic mirror building up a strong quasimonochromatic field while suppressing nonresonant frequencies.

II. DESIGN AND ANALYSIS OF VERTICAL-CAVITY RESONANT THERMAL EMITTER

In this paper we investigate two vertical-cavity enhanced resonant thermal emitter designs; namely with tungsten and with silver as metallic mirrors. The cavity in both designs is made from SiO_2 with a thickness of $L_0 = 0.78$ μm. The 1D
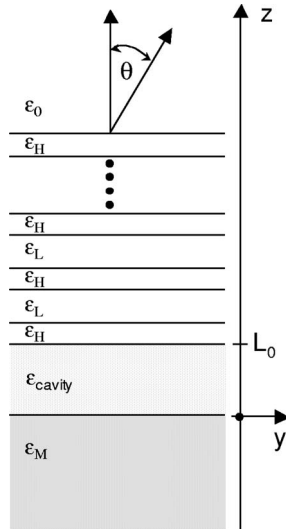
FIG. 1. Cross-sectional view of vertical-cavity enhanced resonant thermal emitter (VERTE).

FIG. 2. Projected band diagram of 1D photonic crystal with a defect state and VERTE projected resonant modes.

PhC, acting as the top mirror, is made out of alternating quarter-wave layers of Si and SiO$_2$ where $d_H=0.17$ μm and $d_L=0.39$ μm are layer thicknesses, respectively. For the time being both Si and SiO$_2$ are considered lossless dielectrics with refractive indices of $n_H=3.34$ and $n_H=1.45$, respectively. We use the shorthand notation where a Si quarter-wave layer is denoted with H (high-refractive index), and a SiO$_2$ quarter-wave layer with L (low-refractive index), and where the system of n pairs of layers can be represented as (HL)^n. In this particular design, the PhC mid-band gap is at $\lambda=2.35$ μm, which approximately determines resonant wavelength of the structure. The cavity and the band-gap design can easily be scaled in the wavelength region of interest allowing for a tunable thermal emitter source.

Thermal emission from a multilayer structure such as VERTE can relatively easily be calculated using the fluctuation-dissipation theorem.[7] Yet, we will use Kirchhoff's law[15] to calculate the directional polarized emittance by means of the directional polarized absorptance. Indeed, emittance ϵ can be expressed as $\epsilon=1-R$ where R is the reflectance of the structure. To calculate the reflectance we use the transfer matrix approach,[16] while for detailed resonant cavity design and parametrization we use lumped parameter models of transmission lines and perturbation theory.[17]

We will initially approach the analysis of the emitter from the photonic crystal perspective using some of the formalisms already developed in the photonic crystal community. To develop understanding of the resonant thermal emission and to further develop the intuition we will use the notion of the projected band diagram of an infinite 1D photonic crystal[18] with a defect state. Indeed, we can treat this geometry as a cavity (double layer) surrounded on both sides by 1D photonic crystal mirrors. The projected photonic band diagram of an infinite 1D PhC composed of alternating quarter-wave layers of Si and SiO$_2$ with one double-layer of SiO$_2$ (defect)—calculated using the BandSolve software package[19]—is shown in Fig. 2. For a given frequency (ω) and parallel wave vector k_y the projected band diagram
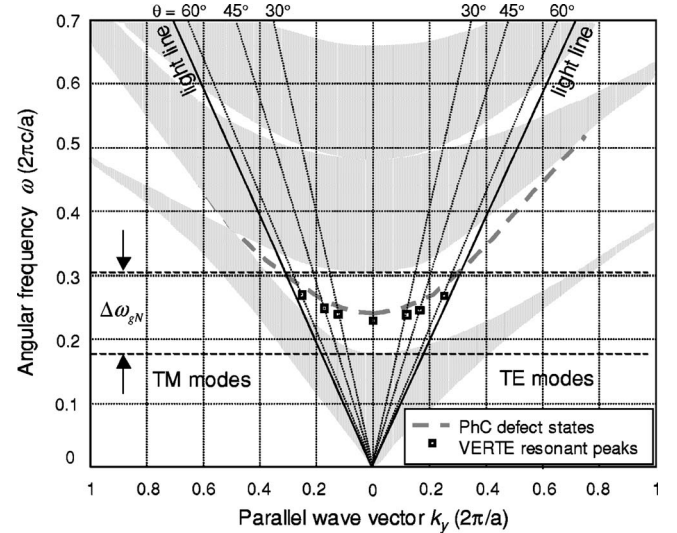
shows whether or not there exists a propagating electromagnetic mode in the z direction. Shaded regions in $\omega-k_y$ space in Fig. 2 designate the existence while white regions designate the absence of propagating modes. The defect in the structure (cavity layer) creates defect states in the band gap, as shown with the dashed line in Fig. 2. We use band-gap defect states as the radiation modes of the structure. Coupling defect states to the free space modes permits far-field resonant radiation that is highly directional, quasimonochromatic thus quasicoherent.

Although an infinite 1D PhC is a useful tool for developing intuition, it is not suitable for practical implementation of thermal radiation sources since dielectric layers are ideally lossless and it would be difficult to locally heat a lossless PhC structure. Therefore we replaced the 1D PhC on one side of the defect with the lossy metallic mirror. The metallic mirror is at the same time a source of thermal radiation (although with very low emittance, typically below 10%) and a cavity mirror. The notion of defect states can still be used, yet one should be cautious. In the band gap, a metallic mirror cannot radiate except through resonant modes. The position of resonant modes is slightly shifted to smaller frequencies due to the complex impedance of a metallic mirror, yet the shape and curvature remain qualitatively the same. Therefore to fully quantify behavior of resonant emission from the VERTE we will analyze the cavity with the use of perturbation theory.[17]

The resonant cavity quality factor, assuming that losses in the cavity are small, can be conveniently expressed as[17]

$$\frac{1}{Q(\theta)} = \frac{1}{Q_I(\theta)} + \frac{1}{Q_E(\theta)}, \quad (1)$$

where Q_I is the internal quality factor related to the power dissipation within the resonant structure, Q_E is the external quality factor that depends on the coupling of the resonator to the outside world, and θ is the angle of incidence. External quality factor is defined as $Q_E=\omega_0 w_T/P_E$ where w_T is the

energy stored in the resonator and P_E is the power lost to the external circuit. Similarly, the internal quality factor is defined as $Q_I = \omega_0 w_T / P_I$ where w_T is the energy stored in the resonator and P_I is the power lost internally in the resonator. At resonance, the cavity reflectance is given as

$$|\Gamma(\theta)|^2 = \frac{Q_I(\theta) - Q_E(\theta)}{Q_I(\theta) + Q_E(\theta)}, \tag{2}$$

and therefore the zero reflectance condition reduces to the condition that the internal and the external quality factors of the cavity must be equal ($Q_I = Q_E$) for a given angle (θ). Indeed, this is true if $P_E = P_I$. This condition can be achieved by adjusting the 1D photonic crystal transmittance (by changing the number of dielectric layers) to be equivalent to the metallic mirror absorptance. The reflectance of a quarter-wave dielectric stack structure designated as $Air - L(LH)^n - L$, near the center of the band gap, for normal incidence [$(\theta) = 0$], and for an odd number of layers can be expressed as

$$|\Gamma|^2 = \left(\frac{n_H \left(\frac{n_H}{n_L} \right)^n - 1}{n_H \left(\frac{n_H}{n_L} \right)^n + 1} \right)^2, \tag{3}$$

while for the structure with an even number of quarter-wave layers designated as $Air - (LH)^n - L$ the reflectance is given as

$$|\Gamma|^2 = \left(\frac{n_L \left(\frac{n_L}{n_H} \right)^n - 1}{n_L \left(\frac{n_L}{n_H} \right)^n + 1} \right)^2. \tag{4}$$

On the other hand, absorption in the metallic layer A_M can be calculated in terms of impedances:

$$A_M = 1 - |\Gamma_M|^2 = 1 - \left(\frac{Z_M - Z_L}{Z_M + Z_L} \right)^2, \tag{5}$$

where Z_M is the impedance of the metallic mirror and Z_L is the impedance of the cavity layer (SiO$_2$). Adjusting the number of layers n in order to get $A_M = 1 - |\Gamma|^2$ results in unity emittance at the resonance. For smaller index contrast between dielectric layers it is easier to fine-tune the number of layers so that $A_M = 1 - |\Gamma|^2$, yet the stop band of the photonic crystal is narrower.

III. NUMERICAL SIMULATION RESULTS

We have designed and simulated two types of vertical-cavity enhanced resonant thermal emitters, namely $Air - H(LH)L^2 - tungsten$ and $Air - H(LH)^2 L^2 - silver$. The normal emittance for the tungsten structure is given in Fig. 3. One can notice the emittance of the near one at the resonance, with full width at half maximum (FWHM) of approximately 51 nm. In comparison with the normal emittance of planar tungsten (given in Fig. 3), the resonant structure has enhanced the emission of the tungsten more than 13 times. Apart from the resonant enhancement, VERTE
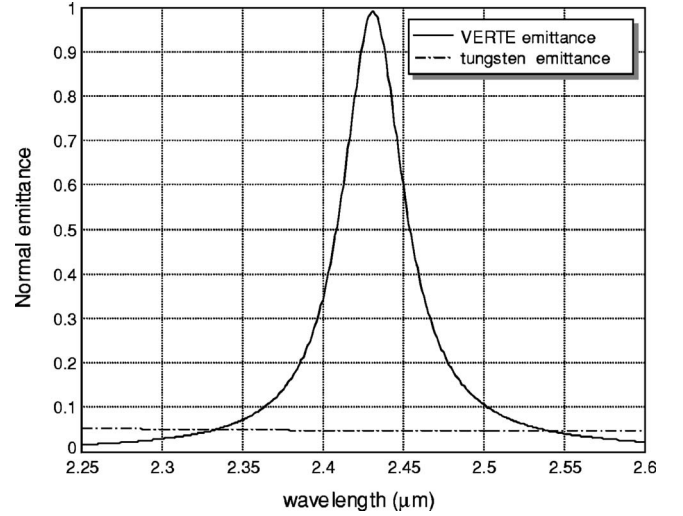

FIG. 3. Normal emittance of vertical-cavity enhanced resonant thermal emitter with tungsten and normal emittance of planar tungsten.

also further suppressed the radiation in the stop band. The normal emittance for the silver structure, given in Fig. 4, exhibits a narrower resonant emittance peak with FWHM of 11 nm, which was expected due to lower losses in the silver resulting in much larger Q of the cavity. Again, notice that the normal emittance of the planar silver in Fig. 4 is enhanced more than 58 times.

In order to gain further insight into the mechanisms of resonant enhancement of thermal emission we simulated the electric field inside the structure that is excited by a normally incident plane wave at the resonance as shown in Fig. 5. One can notice the resonant enhancement of the electric field inside the cavity that leads to increased penetration depth into the metal allowing for near perfect coupling of radiation from VERTE to air.

Another interesting phenomenon is the level of directionality of the emittance for both structures. Polar emittance
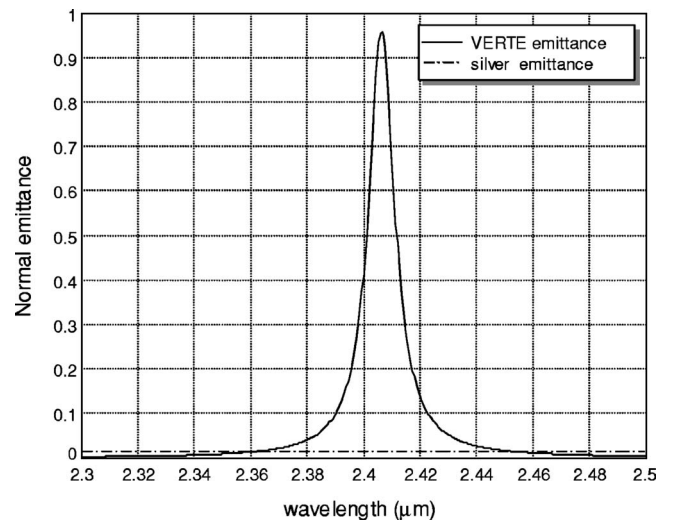

FIG. 4. Normal emittance of vertical-cavity enhanced resonant thermal emitter with silver and normal emittance of planar silver.
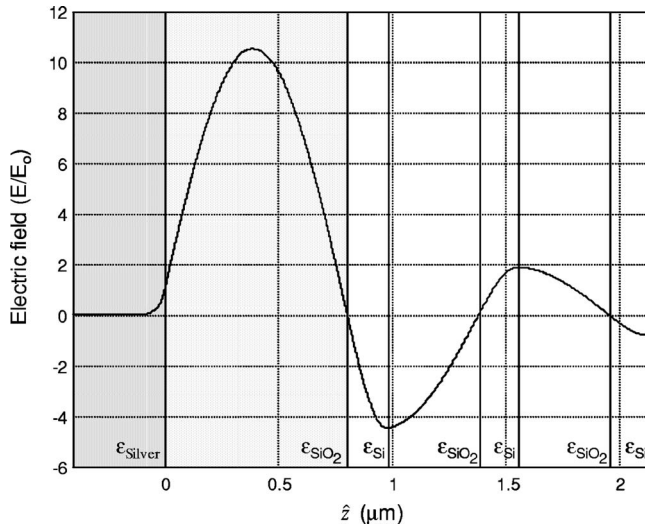
FIG. 5. Normalized electric field in VERTE when excited by plane wave at the resonant frequency.

FIG. 7. Polar plot of silver-VERTE emittance (for TE polarization) at three different wavelengths (2.406, 2.281, and 1.995 μm) corresponding to resonant peak maximums at θ of 0°, 30°(TE polarized), and 60°(TE polarized).

plots at three different wavelengths for silver and tungsten VERTE are shown in Figs. 6 and 7, respectively. Narrow angular lobe emission is even more interesting if we bear in mind that the coherence length of the source is inversely proportional to the angular beam width.[10] Therefore from the angular width of the emission pattern of $\theta=3°$ (for silver VERTE at normal incidence, Fig. 7) we estimate the coherence length of $\lambda/\theta\approx20\lambda$. Since the angular width of the resonant peak is inversely proportional to the quality factor of the cavity, a different material choice and a different operating resonant frequency can provide larger quality factors and consequently even longer coherence lengths. This indeed is an interesting result suggesting that one can engineer temporal and spatial coherence properties of certain thermal sources.

IV. TEMPERATURE SENSITIVITY ANALYSIS

The analysis presented in previous sections used optical properties of dielectrics, semiconductors, and metals at room
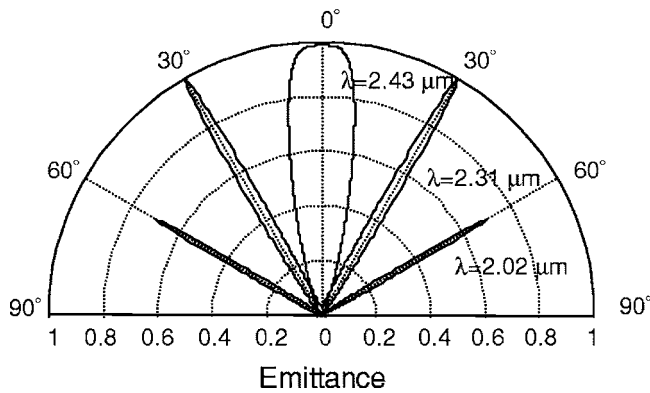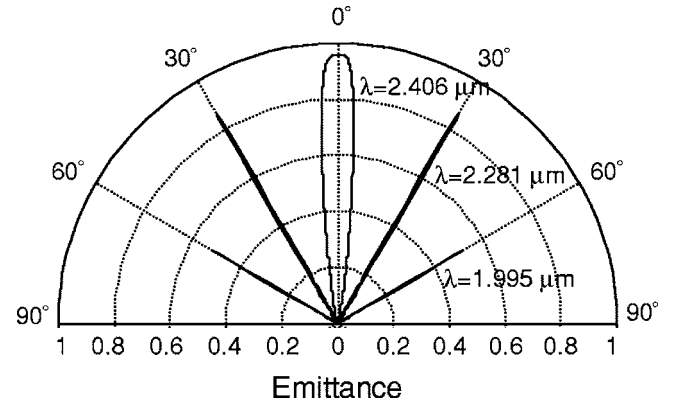

FIG. 6. Polar plot of tungsten-VERTE emittance (for TE polarization) at three different wavelengths (2.43, 2.31, and 2.02 μm) corresponding to resonant peak maximums at θ of 0°, 30°(TE), and 60°(TE). Directional resonant emittance peaks are also designated in Fig. 2 as squares.

temperature and it did not take into account their temperature dependence. The question that naturally arises is how robust the performance of VERTE is with respect to the change in optical properties of the used materials at higher temperatures. In particular, we are interested in estimating optical properties of tungsten, silver, silicon, and silicon dioxide as a function of temperature. Since optical properties of these materials at higher temperatures are not well characterized in the literature, and in some cases different sources report different results, it is very difficult to obtain exact results. Therefore in order to gain better insight into the design robustness we performed sensitivity analysis to establish bounds on performance of the proposed design. First, let us introduce temperature dependent dielectric constants for silver, tungsten, silicon, and silicon dioxide.

Reflectivity of silver, tungsten, and other metals in the IR and near-IR wavelength range is a decreasing function of temperature.[6,20] Therefore the emittance of these materials will increase at high temperatures. To model the temperature dependence of silver and tungsten we use a dielectric function given by the free-electron/Drude model:[20,21]

$$\varepsilon(\omega) = 1 - \left(\frac{\omega_p^2}{\omega(\omega - i\omega_c)}\right), \qquad (6)$$

where ω is the frequency, ω_p is the plasma frequency, and ω_c is the electron collision frequency. Increase in temperature causes the increase of the electron collision frequency (ω_c) thus increasing the absorption in the metal.[20] Plasma frequency ω_p, on the other hand, is approximately modeled as a constant over the range of temperatures.[20] Silver dielectric function is approximately modeled with Eq. (6) where ω_p =8.28 eV, and $\omega_c(T)=[\omega_c(T=300)/300^{1.3}]T^{1.3}$ where $\omega_c(T=300)=0.048$ eV.[20,21]

The temperature dependent absorption in silicon layers is modeled by means of the absorption coefficient as[22,23]

$$\alpha = 4.15 \times 10^{-5}\lambda^{1.51}T^{2.95} \exp\left(\frac{-7000}{T}\right), \qquad (7)$$

where λ is in μm, T is in K, and α is in cm^{-1}, while the refractive index is assumed to be temperature independent ($n_{Si}=3.34$).
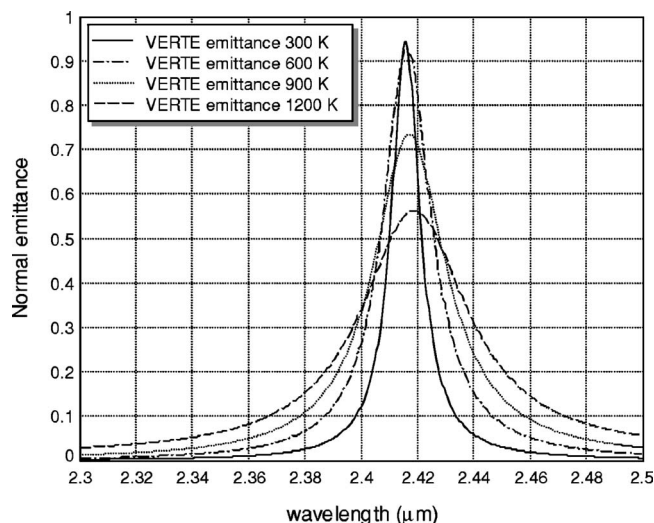
FIG. 8. Normal emittance of VERTE structure $[(LH)^3L^2$–$silver]$ for 300, 600, 900, and 1200 K.

As for the SiO_2, it was shown that the absorption coefficient can be neglected up to 4 μm wavelength, which covers our operating range.[24] Therefore for the purpose of this study it will be assumed that SiO_2 is an ideal dielectric with negligible losses.

Now, we use temperature dependent dielectric functions for numerical simulations of the temperature dependent emittance of VERTE. The normal emittance of $(LH)^3L^2$–$silver$ structure at 300, 600, 900, and 1200 K is given in Fig. 8 (notice that in order to compensate for increased cavity losses we added an additional L layer). Normal emittance of VERTE decreases as the temperature increases due to the increase in the cavity losses. Resonant peak spreading can be observed in Fig. 8 as well, which is caused by the reduction of the internal quality factor of the cavity. However, the emittance change is relatively small and the resonant nature is well preserved even at these temperatures. For a given operating temperature and resonant wavelength VERTE can be optimized to exhibit unity emittance by adjusting the number of PhC layers and/or the index contrast of dielectric materials used.

It should be pointed out that we observed the resonant emission peak shift towards longer wavelengths as the operating temperature is increased. This anomaly is due to the increase in the skin depth of the underlaying silver layer which increases the effective resonant cavity length and shifts the resonant mode towards longer wavelengths.

V. CONCLUSIONS

In conclusion, we have demonstrated a different kind of tunable, quasicoherent, narrow-band thermal radiation source that is suitable for the near-IR and IR range. We have proposed a thin-film structure—based on a vertical cavity and one-dimensional photonic crystal—and demonstrated (by numerical simulation) a narrow angular emission lobe at the designed wavelength with near unity emittance at the resonance. Furthermore, we have demonstrated that we can enhance the directional emittance of a low-emittance material to unity using the vertical cavity concept. We have also concluded that the temperature dependent emittance of the proposed structure does not significantly deviate from the room temperature emittance. We have also observed the shift of the emittance peak towards longer wavelengths as the temperature is increased, which appears to be counterintuitive from the blackbody radiation point of view.

Although, resonant-antennalike thermal emission has been observed before, we present a tunable, quasicoherent, narrow-band thermal emission source based on a thin-film structure. Near-IR and mid-IR light sources are used in a variety of gas sensors, chemical analyzers, and spectrophotometric devices. However, VERTE as a very narrow-band tunable source holds great potential to make these devices smaller, more efficient, and more sensitive. It paves the way towards further integration and miniaturization of on-chip sensors and infrared sources. On a different note, this is another example of how submicron structures interact with thermal radiation creating new radiation patterns, increasing coherence length, and changing the widely accepted notion of incoherent, isotropic, and broadband thermal radiation sources.

*Email address: ivanc@mit.edu

[1] E. Yablonovitch, Phys. Rev. Lett. **58**, 2059 (1987).

[2] C. M. Cornelius and J. P. Dowling, Phys. Rev. A **59**, 4736 (1999).

[3] M. Scalora, M. J. Bloemer, A. S. Pethel, J. P. Dowling, C. M. Bowden, and A. S. Manka, J. Appl. Phys. **83**, 2377 (1998).

[4] A. Narayanaswamy and G. Chen, Phys. Rev. B **70**, 125101 (2004).

[5] H. Sai, H. Yugami, Y. Akiyama, Y. Kanamori, and K. Hane, J.

Opt. Soc. Am. A **18**, 1471 (2001).

[6] H. Sai, T. Kamikawa, Y. Kanamori, K. Hane, H. Yugami, and M. Yamaguchi, in *Proceedings of the Sixth NREL Conference on Thermophotovoltaic Generation of Electricity*, AIP Conf. Proc. No. 738 (AIP, New York, 2004), pp. 206–214.

[7] C. Luo, A. Narayanaswamy, G. Chen, and J. D. Joannopoulos, Phys. Rev. Lett. **93**, 213905 (2004).

[8] S. Y. Lin, J. G. Fleming, D. L. Hetherington, B. K. Smith, R.

Biswas, M. M. S. K. M. Ho, W. Zubzycki, S. R. Kurtz, and J. Bur, Nature (London) **394**, 251 (1998).

[9] J. G. Fleming, S. Y. Lin, I. El-Kady, R. Biswas, and K. M. Ho, Nature (London) **417**, 52 (2002).

[10] J. J. Greffet, R. Carminati, K. Joulain, J. P. Mulet, S. Mainguy, and Y. Chen, Nature (London) **416**, 61 (2002).

[11] F. Marquier, K. Joulain, J. P. Mulet, R. Carminati, and J. J. Greffet, Opt. Commun. **237**, 379 (2004).

[12] M. U. Pralle, N. Moelders, M. P. McNeal, I. Puscasu, A. C. Greenwald, J. T. Daly, E. A. Johnson, T. George, D. S. Choi, I. El-Kady, and R. Biswas, Appl. Phys. Lett. **81**, 4685 (2002).

[13] P. Ben-Abdallah, J. Opt. Soc. Am. A **21**, 1368 (2004).

[14] D. G. Deppe and C. Lei, Appl. Phys. Lett. **60**, 527 (1992).

[15] J. J. Greffet and M. N. Vesperinas, J. Opt. Soc. Am. A **15**, 2735 (1998).

[16] E. Hecht, *Optics*, 4th ed. (Addison-Wesley, San Francisco, CA, 2002).

[17] D. H. Staelin, A. W. Morgenthaler, and J. A. Kong, *Electromagnetic Waves*, 2nd ed. (Prentice-Hall, Upper Saddle River, NJ, 1994).

[18] J. N. Winn, Y. Fink, S. Fan, and J. D. Joannopoulos, Opt. Lett. **23**, 1573 (1998).

[19] *Bandsolve 1.0* (RSoft Design Group, Inc., Ossining, NY, 2002).

[20] K. Ujihara, J. Appl. Phys. **43**, 2376 (1972).

[21] A. D. Rakic, A. B. Djurisic, J. M. Elazar, and M. L. Majewski, Appl. Opt. **37**, 5271 (1998).

[22] P. Vandenabeele and K. Maex, J. Appl. Phys. **72**, 5867 (1992).

[23] P. J. Timans, J. Appl. Phys. **74**, 6353 (1993).

[24] M. F. Modest, *Radiative Heat Transfer*, 2nd ed. (Academic Press, San Diego, CA, 2003).